공학석사 학위논문

Anticoagulating nanofilm coating for pancreatic islet cell transplantation

췌도 세포 이식용 항응고 나노필름 코팅 개발

2023 년 2 월

서울대학교 대학원

협동과정 바이오엔지니어링 전공

이동현

공학석사 학위논문

Anticoagulating nanofilm coating for pancreatic islet cell transplantation

췌도 세포 이식용 항응고 나노필름 코팅 개발

2023 년 2 월

서울대학교 대학원

협동과정 바이오엔지니어링 전공

이동현

Anticoagulating nanofilm coating for pancreatic islet cell transplantation

지도 교수 황 석 연

이 논문을 공학석사 학위논문으로 제출함

2022년 12월

서울대학교 대학원

협동과정 바이오엔지니어링 전공

이동현

이동현의 공학석사 학위논문을 인준함

2023년 2월

위 원 장 _____(인)

부위원장 _____(인)

위 원 _____(인)

ABSTRACT

Anticoagulating nanofilm coating for pancreatic islet cell transplantation

DongHyun Lee

Interdisciplinary Program in Bioengineering

The Graduate School of Engineering

Seoul National University

A major limitation of pancreatic islet transplantation is pancreatic function loss caused by immediate immune rejection reaction within 3 days after transplantation. To prevent the immediate destruction of pancreatic islets after transplantation, it is necessary to alleviate the Instant Blood-Mediated Inflammatory Reaction (IBMIR) and suppress the immune system. In this study, sulfated polymers were selected as anticoagulating nanofilm materials for their anticoagulating and anti-inflammatory effects. Monophenol was conjugated to polymers, and hydrogel nanofilms were crosslinked through an oxidation coupling reaction of monophenols via Tyrosinase derived from *Streptomyces avermitilis* (SA-Ty) to increase nanofilm stability. Anticoagulating hydrogel nanofilm was coated on the surface of pancreatic β-cell spheroids to provide protection from blood coagulation and IBMIR that occur in the

early stages of transplantation. The anticoagulating effect was evaluated by measuring platelet adhesion and thrombin activity in the blood. The newly developed anticoagulating hydrogel nanofilm did not affect the gene expression of β-cell spheroids and insulin secretion ability. These coated spheroids were transplanted into an *in vivo* rat model, and engraftment of coated spheroids and anticoagulant effects were evaluated. Overall, it is expected that the anticoagulating hydrogel nanofilm developed in this study will be effective in intrahepatic pancreatic islet transplantation for the treatment of Type 1 Diabetes.

Keywords: IBMIR, Heparin, Coagulation, Transplantation, Islet, 3D cultures.

Student Number: 2021-27001

Table of Contents

List of Figures and Table

Figures

Tables

Chapter 1. The Study Scientific Background and Purpose of Research

1.1 The Study Scientific Background

1.1.1 Cell Transplantation

A person's ability to restore damaged tissue to its original state after injury is greatly limited [1]. As a method to treat damaged tissues and certain diseases, cell therapy aims to regenerate damaged tissue or replace the function of damaged tissue by transplantation of stem cells, T-cells, and pancreatic β-cells [2-4]. Complete restoration of tissue is a goal that regenerative medicine hopes for. But there are several limitations in cell transplantation for tissue regeneration. First, survival rate of transplanted cells is very low. Second, the rate of engraftment in the transplantation site is low. Third, immune rejection by the recipients occurs in the case of allogeneic or xenogeneic cell transplantation [5]. Cell transplantation utilizing biomaterials is a promising method to solve these problems [6]. Hyaluronic acid is often used to increase cell survival by preventing cell death caused by mechanical stress that occurs during cell injection [7]. In addition, patch-type hydrogels produced using gelatin methacrylate (GelMA) and polyethylene glycol diacrylate (PEGDA) has been developed for cell implantation [8]. As such, it is necessary to study methods for solving problems that occur during cell transplantation for tissue regeneration.

1.1.2 Type 1 Diabetes

Type 1 Diabetes is a disease in which the pancreatic β-cells, which are responsible for insulin secretion, are destroyed by autoimmune diseases, and thus blood glucose levels cannot be controlled [2, 9, 10]. Type 1 Diabetes is known to account for 5 to 10% of all diabetic patients and is often diagnosed in childhood [11]. As an alternative treatment strategy to daily insulin injection, islet transplantation has been increasingly used since the development of Edmonton protocol, which is a surgical method of transplanting isolated islets to the liver through the portal vein [2, 12, 13]. However, despite the establishment of the transplantation method, problems such as 1) lack of pancreatic donors, 2) insufficient oxygen and nutrients supply to engrafted islets, and 3) foreign body immune responses after transplantation have yet remained to be solved [14-16]. Therefore, solutions, such as 1) stem cell-derived *β*-cell transplantation and 2) protection of islets from the immune response through encapsulation are being proposed [3, 17]. As one of islet encapsulation strategies, polymers with different charges can be applied to islet surface through Layer-by-Layer (LbL) coating resulting in the encapsulation of islet in a nanometer thickness [18]. Nanoencapsulation technology has the advantage of small graft size and allows encapsulated islets to be successfully transplanted via the portal vein, which is currently performed clinically.

1.2 Purpose of Research

Instant Blood Mediated Inflammatory Reaction (IBMIR) is a significant problem when islets contact the donor's blood after being infused to a intraportal vein, leading to islet graft failure [19]. Therefore, nanoencapsulation methods that enable nutrient/waste exchange, long-term blood glucose control, and inhibit IBMIR are highly desired. In a previous study, an enzymatically crosslinked LbL hydrogel nanofilm encapsulation platform was established by conjugating monophenols in Glycol Chitosan (GC) with amine functional group and Hyaluronic Acid (HA) with carboxyl group functional group [20]. Hydrogel nanofilm encapsulated β-cell spheroids were transplanted to kidney capsular space of Type 1 Diabetic mouse and regulated blood glucose levels for long term without immunosuppressant. In this study, polymers were selected as candidates based on the degree of sulfation for anti-inflammatory and anticoagulant effects of the sulfate group [21]. Sulfated polymers with an anticoagulating effect can be applied to previously established enzymatic crosslinking cell coating platforms by conjugation of the monophenol group to the carboxyl group of polymers. This research aims to prevent IBMIR and blood coagulation reactions in the early stage of transplantation by utilizing anticoagulating materials in LbL cell coating technique.

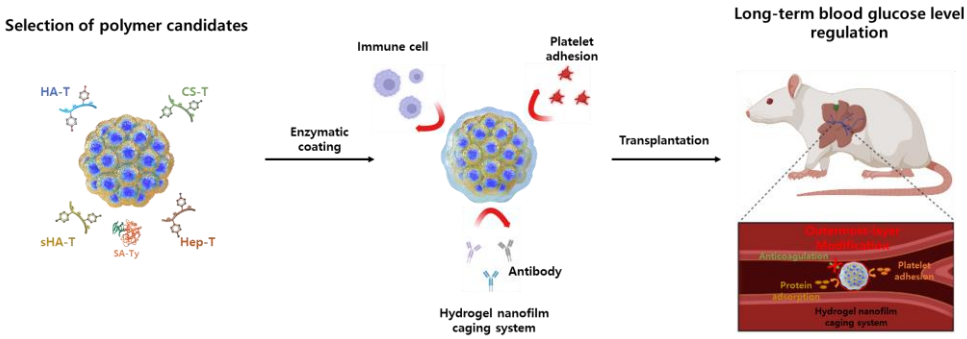

Figure 1.1 Overview of anticoagulating nanofilm coating for pancreatic islet cell transplantation.

Chapter 2. Anticoagulant polymer selection and effect evaluation for pancreatic β cell spheroids

2.1. Materials and methods

2.1.1 Materials

Glycol chitosan (Degree of Deacetylation 80%, MedChemExpress), Sodium Hyaluronic acid (41KDa-65KDa, Lifecore Biomedical), Chondroitin sulfate A sodium salt from bovine trachea (Sigma-Aldrich), Heparin sodium salt (15kDa, MedChemExpress) was used.

2.1.2 Synthesis of monophenol conjugated polymers

To synthesize monophenol-linked glycol chitosan (GC-T), 4-Hydroxyphenylacetic acid (HPA; Sigma-Aldrich) and glycol chitosan (GC) were conjugated using 4-(4,6-dimethoxy-1,3,5-triazin-2-yl)-4-methyl-morpholinium chloride (DMTMM; Tokyo Chemical Industry). First, 200mg of GC was added to 10ml 2-(*N*-morpholino) ethane sulfonic acid (MES) buffer pH 5.5 (Thermo Fisher) and dissolved using ultrasonication for about 1 min, and then stored at 60 °C for complete dissolution. HPA was completely dissolved in 10ml MES buffer at 70°C and then reacted at 70°C for 20 min after adding DMTMM. Then, dissolved GC was added to reacted HPA solution. The mixture was reacted for 2 hours at 70°C and then reacted overnight at RT. After the reaction was completed, the solution was placed in a dialysis tube (SnakeSkin™ Dialysis Tubing, Mw cutoff 3.5 kDa, Thermo Fisher Scientific) and dialyzed against Deionized Water (DW) for 72 hours. DW was changed every 3 hours or 6 hours. After dialysis, freeze-drying was performed for 72 hours.

Monophenol-conjugated hyaluronic acid (HA-T) was produced by conjugating hyaluronic acid (HA) and tyramine hydrochloride (Sigma-Aldrich) through 1-Ethyl-3-(3-dimethylaminopropyl) carbodiimide (EDC; Thermo Fisher) and N-Hydroxysuccinimide (NHS; Sigma-Aldrich) reactions. HA, EDC, NHS, and Tyramine hydrochloride were added in a 1:2:2:4 molar ratio. First, 200 mg of HA was dissolved in 20 ml MES buffer, and EDC was added after HA was completely dissolved and reacted for 30 min at RT. After 30 min reaction, NHS was added and reacted for 30 min at RT. Finally, the reacting sample and tyramine hydrochloride were allowed to react overnight at RT. After the reaction was completed, dialysis and freeze-drying were performed.

Tyramine hydrochloride was crosslinked to chondroitin sulfate (CS), sulfated hyaluronic acid (sHA), and Heparin (Hep) using the same method. sHA was synthesized through an additional process based on patents. (IT. Patent No. 10-2018-0082454, (2016)). To conjugate Rhodamine B isothiocyanate (RITC; Sigma-Aldrich) or Fluoresceinamine isomer I (FA; Sigma-Aldrich) to the polymers, RITC and FA were dissolved in *N, N* Dimethylformamide (DMF) in 10mg/ml. Then, 1ml of the dissolved solution was added to the reaction solution of GC-T, HA-T, sHA-T, CS-T, and Hep-T to obtain GC-T-RITC, HA-T-FA, sHA-T-FA, CS-T-FA, and Hep-T-FA respectively.

2.1.3 Expression and Purification of recombinant tyrosinase derived from Streptomyces avermitilis (SA-Ty)

A recombinant plasmid for tyrosinase production was provided by Professor Byung-Gee Kim (Seoul National University, Seoul). Tyrosinase (Ty) used in this study is a

recombinant tyrosinase derived from Streptomyces avermitilis (SA) and has a His-tag introduced at the C-terminus of Ty. First, the plasmid for SA-Ty expression was transformed into E. coli BL21(DE3) by heat shock. E. coli was selectively screened by plating on Luria-Bertani (LB) agar plates containing 100 μg/ml ampicillin. Selected colonies were amplified in 3 ml of LB medium containing ampicillin with 100 μg/ml ampicillin and cultured overnight at 37° C. and 200 rpm. Then, 3 ml of the sufficiently expanded cell culture was inoculated into 200 ml LB containing 100 μg/ml ampicillin. When the cells were cultured for 3 hours, they were grown to OD600. SA-ty expression was then induced by adding 0.05 mM IPTG and 1 mM CuSO4. After incubation for 20 hours at 18° C. and 200 rpm for sufficient expression, the cells were collected by centrifugation at 4° C. and 6,000 rpm for 10 minutes. The centrifuged cell pellet was washed three times with 50 mM Tris-HCl buffer (pH 8.0) to remove the remaining culture medium. The cells were lysed by ultrasound and the proteins in the cells were obtained. Cell lysates were centrifuged at 15,000 rpm for 30 min at 4 °C to sediment the unwanted cell suspension. Several proteins were collected from the supernatant and His-tagged SA-Ty was purified using a Ni-NTA agarose column (QIAGEN). Purified tyrosinase was filtered through a sterile 0.45 μm polyethersulfone membrane (Acrodisc® Syringe Filter with Supor® Membrane, Fall Life Sciences, USA) and diluted 1:1 in pH 8.0 Tris-HCl buffer containing 75% glycerol. The concentration of the produced tyrosinase was quantified using the Bicinchoninic Acid (BCA) Protein Assay Kit (Thermo Fisher Scientific).

2.1.4 NMR analysis

Freeze-dried samples were dissolved in D_2O. Then ^1H NMR spectra were detected

by AvanceIII HD (Bruker, German) 300 MHz spectrometer.

2.1.5 Fourier transform infrared (FTIR) spectroscopy analysis

To confirm the enzyme reactivity to SA-Ty, 0.1% GC-T and 0.1% HA-T solutions were reacted with 0.05 U/ml SA-Ty at RT for 30 minutes. Thereafter, the reaction solution was dialyzed against DW for 24 hours, and DW was changed every 3 hours or 6 hours and freeze-dried after dialysis. Solid samples were measured on crystal crystals of FTIR (TENSOR27, Bruker, Germany). FTIR spectrum were scanned and analyzed for transmittance from 400-4000 cm^{-1}.

2.1.6 Measurement of zeta potential and enzyme activity

To measure zeta potential, synthesized materials were dissolved in DW to a concentration of 1mg/ml. Zeta potential of the materials was measured using Nano ZS (Malvern Instruments, Germany). Substrate [0.1% (w/v) Monophenol synthesized polymer, 200 μM l-tyrosine] SA Ty (0.05 U/ml) and 10 μM $CuSO_4$ were reacted in a 200 μl volume of 50 mM Tris-HCl buffer (pH 8.0) to obtain enzyme activity. To confirm the enzymatic substrate reaction of SA-ty, absorbance at 475 nm was measured every minute for 60 minutes at 37 °C. Absorbance was measured after a 10-minute reaction based on previous studies.

2.1.7 Cell culture

MIN6 cells were cultured using high-glucose Dulbecco's Modified Eagle's medium (DMEM; Hyclone) containing 15% fetal bovine serum (FBS; Gibco), 1% PS penicillin/streptomycin (P/S; Gibco), and 55 μM 2-Mercaptoethanol (2-ME; Thermo)

at 37°C, 5% CO2 incubator. The medium was changed every 2 days. For subculture or spheroids formation, MIN6 cells were detached from the culture plate using 0.25% trypsin-EDTA (Gibco), and the cells were harvested by centrifugation at 1100 rpm for 3 minutes. To produce MIN6 spheroids, cells were seeded in 2.5×10^3 cells/well density in ultra-low attachment round bottom 96 well plate (Corning) or 1.2×10^6 MIN6 cells were seeded in AggreWell™400 Microwell Culture Plates (STEMCELL Technologies Inc) according to manufacturer's instruction. The seeded cells were incubated for 3-4 days.

2.1.8 Cell hydrogel nanofilm coating

MIN6 spheroids were encapsulated with a hydrogel nanofilm through an enzyme crosslinking-based caging system. Spheroids produced with ultra-low attachment round bottom 96 well plate or AggreWell™400 Microwell Culture Plates were collected in a 15 ml vertical tube and washed twice with DPBS (DULBECCO'S PHOSPHATE BUFFERED SALINE; biowest). 100 spheroids were placed in 8.0 μm polycarbonate membrane Transwell 6.5-mm inserts, and the inserts were transferred to 24-well plates (Corning). 600ul of GC-T solution (1 mg/ml) and SA-Ty (0.05 U/ml) were added to a well in a 24-well plate. Then, the Transwell inserts with spheroids were placed in the well with GC-T and SA-Ty solution and incubated at 37°C, 5% CO2 incubator for 10 min. The 24-well plate was tapped every two minutes for better diffusion. After 10 minutes, the Transwell was transferred to the next well with 600 μl culture medium and incubated for 30 seconds. Then, the Transwell was transferred to the next well with 600 μl DPBS and incubated for 1 minute. This step was repeated once. In the same method, HA-T and GC-T were

alternately applied up to 5 layers. Candidate materials (HA-T, sHA-T, CS-T, Hep-T) were applied in the last layer (sixth layer) using the same method. After encapsulation, MIN6 spheroids were washed twice with DPBS and transferred to a sterile 35mm plate containing culture medium.

2.1.9 Cell viability

Cells were stained and identified with Live/Dead® Viability/Cytotoxicity Kit (Invitrogen) containing Calcein-AM and EthD-1 (EthD-1) to determine cell viability. Cell viability after layer-by-layer coating was confirmed by imaging with a fluorescence microscope (EVOS® Cell Imaging Systems, Thermo Fisher Scientific).

2.1.10 Coating stability

To evaluate the coating stability, the last layer of the coating platform was coated using 0.1%(w/v) HA-T-FA, sHA-T-FA, CS-T-FA, and Hep-T-FA. Starting from Day 1 after coating, the fluorescence intensity was imaged for about a week every two days using a fluorescence microscope (EVOS® Cell Imaging Systems, Thermo Fisher Scientific).

2.1.11 Coagulation test of material and coated beads

Each material was dissolved in a concentration of 0.1%(w/v) in rat plasma with sodium citrate (Innovative Research). Coagulation was started by adding 50 mM $CaCl_2$ in DPBS. The absorbance was measured every 1 min for 1 hour at a wavelength of 405 nm. 20 mg Polymethylmethacrylate (PMMA) beads (Cospheric) were coated with GC-T (1 mg/ml) in DPBS solution with SA-Ty (0.05U/ml) for 10

min, washed through DPBS, and HA-T (1 mg/ml) was coated in the same way. In a repeated manner, PMMA beads were coated with 6 layers of GC-T and HA-T. The coagulation reaction was then observed in the same manner above.

2.1.12 SEM (Scanning Electron Microscope)

Glass or silicon wafer (1.7cm * 1.7cm) was prepared and cleaned using piranha solution for 15 minutes. Piranha solution was made in a 3: 1 ratio of sulfuric acid (H_2SO_4) and hydrogen peroxide (H_2O_2). PDMS(SYLGARD 184 Base & Curing Agent 500g KIT; Dow corning) mold was produced at a 10:1 ratio and incubated at 60°C overnight. A punch (3 mm) was used to make a hole in the mold, and the mold was attached to the glass or silicon wafer. 0.5% (w/v) of GC-T and SA-Ty (0.05U/ml) was treated to the glass or silicon wafer with PDMS mold for reaction overnight at RT. The glass and silicon wafer coated with GC-T was washed with DPBS. Then, 0.5% (w/v) HA-T or 0.5% (w/v) Hep-T was applied with SA-Ty (0.05U/ml) in the same manner. Single Donor Human Whole Blood anticoagulated with Na Citrate (Innovative Research) was centrifuged at 2000xg for 12 minutes to achieve Platelet-rich plasma. Platelet-rich plasma was applied to GC-T/HA-T or GC-T/Hep-T coated glass or silicon wafer to react for 2 hours. After the reaction, the glass or silicon wafer was washed twice with DPBS and fixed using 2.5% EM Grade AQUEOUS GLUTARALDEHYDE (EMS) for 30 minutes. Sequential dehydration was carried out with 50%, 70%, 80%, and 90% EtOH for 10 min. Then, samples were washed twice using 100% EtOH. The samples were then completely dried using HMDS and imaged using SEM (FE-SEM 7800F Prime). Spheroids made using AggreWell™ 400 Microwell Culture Plate were reacted with blood for 30 min. After 30 minutes,

the spheroids were obtained from the blood, fixed, and dehydrated in the same manner as mentioned above. The spheroids were completely dried and imaged using SEM.

2.1.13 Thrombin activity measurement

Experiments were conducted using spheroids made using AggreWell™ 400 Microwell Culture Plates. The spheroids were reacted with human blood for 30min or 1 hour. Then, the blood with spheroids was centrifuged at 2500xg for 25min to obtain the plasma. Thrombin Activity was measured at 490mm/520mm according to the protocol from SensoLyte 520 Thrombin Activity Assay Kit *Fluorometric*. Plasma samples were used after 5-fold dilution.

2.1.14 Real-time PCR

24 hours after *β*-cell spheroids were coated, *β*-cell spheroids were collected in 1.7 ml EP tube and washed with DPBS. RNA ISO reagent was treated to the coated β-cell spheroids and vortexed for about 10 seconds to prepare the sample for RT-PCR. RNA extraction was performed according to the manufacturer's instructions using the easy-spin™ Total RNA Extraction Kit (IntronBio, Korea). After measuring the RNA concentration, cDNA was prepared by reverse transcription according to the manufacturer's instructions using EZ006M kit 110 (Enzynomics, Korea) according to the RNA concentration. Gene expression levels of pancreatic β-cell functional markers GLUT-2, insulin-1 (Ins1), and insulin-2 (Ins2) were identified using SYBR green PCR Mastermix and StepOnePlusTM Real-Time PCR (Applied Biosystems). To normalize gene expression level, glyceraldehyde-3-phosphate dehydrogenase

(GAPDH) was chosen for housekeeping gene.

2.1.15 Insulin secretion of beta cell via glucose stimulation

The cellular function of MIN6 β-cells was confirmed through the level of insulin secretion. β-cell spheroids were washed twice with DPBS and incubated in 1 ml (2 mM glucose in Krebs-Ringer solutions) for 1 hour at 5% CO2, 37°C. After 1 hour, the cells were alternately treated with a low-glycemic solution (3.3 mM glucose in Krebs-Ringer solutions) and a high-glycemic solution (20 mM glucose in Krebs-Ringer solutions) and incubated in a 37°C incubator for 1 hour each. The supernatant of the glucose solution containing the insulin protein secreted from the spheroids was collected from each well. Insulin levels were measured using Mouse Insulin ELISA kit (ALPCO, NH, USA). β cell spheroids were lysed by ultrasonication in RIPA buffer for 15 min, followed by vortexing on Ice for an additional 15 min every 5 min. BCA assay analysis was performed to quantify cellular proteins in whole spheroids as a way to normalize secreted insulin levels. The stimulation index (SI) was calculated as the amount of insulin under the hyperglycemic condition divided by the amount of insulin under the hypoglycemic condition.

2.1.16 β cell spheroid transplantation

MIN6 insulinoma cells were formed into spheroids (1000 cells per spheroid) and coated as discussed above. Before transplantation, coated spheroids in 15ml conical tubes were stored in culture media. The spheroids were placed into the syringe with 3 ml of DPBS, and the syringe (Korea Vaccine) inlet. Rats (F344) were anesthetized

by isoflurane exposure. After the rats were successfully anesthetized, abdominal hair was removed using shaver. Abdominal incision was made using scissor in order to expose the ileocolic vein. The fat around the blood vessels was removed for injection of catheter into blood vessel. Blood vessels are pre-sealed with a suture needle and prepared for transplantation. The catheter was inserted into the blood vessel. Then, prepared DPBS (sham), uncoated spheroids (native), and crosslinked spheroids (Hep-T) was injected through catheter (3000uL per rat). When the injection was finished, the catheter was removed, and the blood vessel was sutured to prevent excessive blood loss. The incision was closed with sutures. Blood was collected at 15 minutes after infusion of spheroids, and plasma was separated at 10000xg for 2 minutes. After 3 days, rats were anesthetized with isoflurane for liver resection and blood collection. After hair removal, the liver was exposed through an abdominal incision. Rats were euthanized after 5 ml of blood was collected. The liver was cut with surgical scissors into appropriate sizes and fixed in 4% PFA (paraformaldehyde).

2.1.17 Thrombin activity measurement

The concentration of thrombin-anti-thrombin complex (TAT) was measured using Rat Thrombin-antithrombin (TAT) complexes ELISA Kit (Colorimetric) (Novus Biologicals, USA) according to manufacturer's protocol. Experiments were conducted using plasma separated from blood collected 15 minutes after transplantation with EDTA as anticoagulant. Plasma samples were used after 5-fold dilution.

2.1.18 Histological analysis of liver sections

After liver tissues were fixed in 4% PFA for 1 day, the sliced livers were placed in tissue cassettes and residual PFA was removed in running tap water for 1 day. The liver was dehydrated for 30 minutes in the order of 70%, 80%, 95%, 100% Ethanol and infiltrated in xylene for 2 hours and paraffin for 1 day. Tissues were infiltrated with paraffin for 1 day in a paraffin embedding machine, solidified in a paraffin block, and sectioned at 5μm thickness using a microtome. After dehydration, tissues were stained with hematoxylin and eosin stains (H&E). Stained tissue was examined under a microscope.

2.1.19 Statistical analysis of experiments

Experiments were carried out for at least three trials for statistical analysis. Data are expressed as mean ± standard deviation. Statistical significance of the outcome values was determined by paired student's t-test and one way ANOVA with *$P < 0.05$, ** $P < 0.01$, and *** $P < 0.005$.

2.2. Result & Discussion

2.2.1 Synthesis of Materials and Characterization

EDC/NHS activation mechanism and DMTMM amide coupling were used to introduce monophenol groups into glycol chitosan (GC) and hyaluronic acid (HA), sulfated hyaluronic acid (sHA), chondroitin sulfate (CS), and heparin (Hep). EDC/NHS activation reaction is a method for coupling a carboxylic acid group with an amine group. The carboxylic acid group is activated via EDC and becomes unstable. Then, activated carboxylic acid reacts with NHS to reach a stable state. (Figure 2.1). The amine group is then replaced with the NHS to form an amide bond. 4-Hydroxyphenylacetic acid (HPA), a monophenol with a carboxyl functional group, was used for the GC group, and Tyramine hydrochloride (Tyr), a monophenol with an amine functional group, was used for HA. GC, DMTMM, and HPA were reacted in a 1:4:4 molar ratio, and HA, sHA, CS, and Hep were reacted in a 1:2:2:4 molar ratio with EDC, NHS, and Ty (Table 1.). In the previous study, Tyramine conjugated HA was named HA-T. Therefore, newly synthesized materials were similarly named by adding ' T ' to indicate the conjugated mono-phenol group [22-24].

^{1}H–nuclear magnetic resonance spectra of GC-T, HA-T, sHA-T, CS-T, Hep-T showed peaks at 6.8 – 7.5 parts per million (ppm) which are corresponding to the protons of phenols (Figure 2.2A-E). HA-T showed peak at 2.0 ppm indicating acetyl methyl protons, and GC showed peak at 2.5 – 3.0 ppm indicating second carbon of GC (Figure 2.2A-E). The degree of substitution (DS) was calculated by comparing the relative peak integration ratios using the following equation: (1)(2)

$$DS(\%) = \frac{\frac{1\,Tyr}{4}}{\frac{1\,HA}{3}} * 100 \qquad (1)$$

$$DS(\%) = \frac{\frac{1Tyr}{4}}{1GC*\frac{100}{80}} * 100 \qquad (2)$$

DS of GC-T, HA-T, sHA-T, CS-T, and Hep-T was 16.59%, 24.58%, 14.06%, 14.35%, and 22.19% respectively (Table 2.). The zeta potentials of 0.1% GC-T, 0.1% HA-T, 0.1% sHA-T, 0.1% CS-T, 0.1% Hep-T solution were 1.56 ± 0.234 mV, and -21.7 ± 1.37 mV, -27.6 ± 0.666 mV, -35.2 ± 1.77 mV, -30.9 ± 1.53 mV, respectively (Figure 2.3).

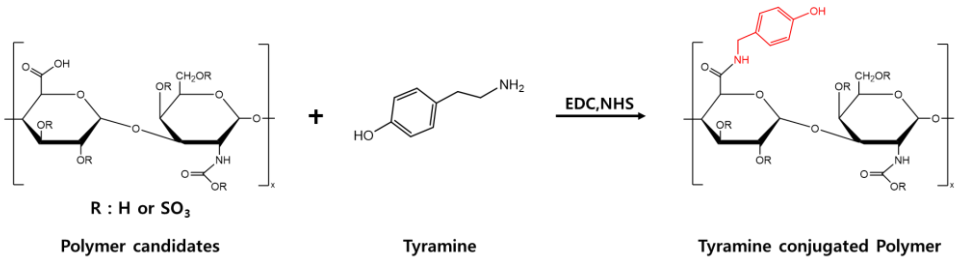

Figure 2.1 Tyramine conjugation to polymer candidates.

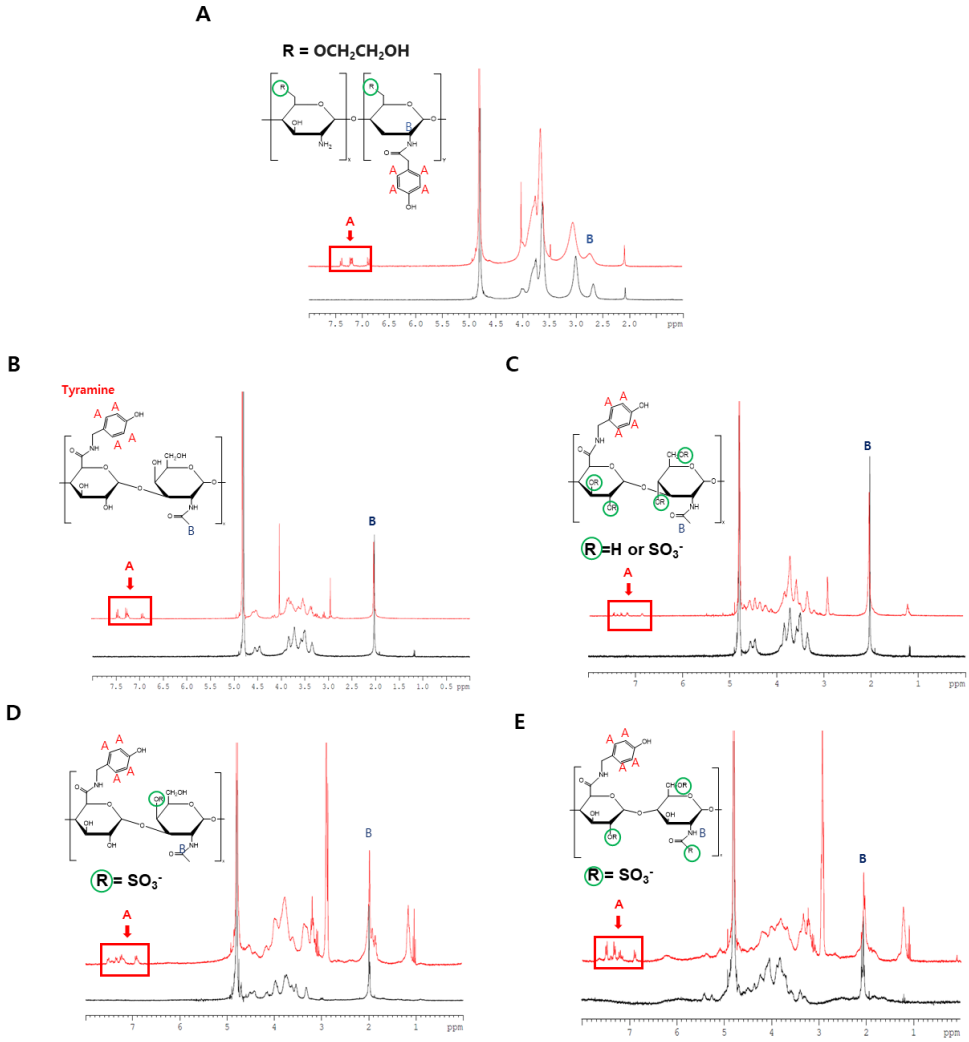

Figure 2.2 Synthesis of materials and characterization.

1H NMR spectra of synthesized polymers obtained on a 300 MHz NMR spectrometer (A: Tyramine peak, B: Acetyl peak). Degree of substitution of the synthesized (A) GC-T: 16.59% (B) HA-T: 24.58% (C) sHA-T: 14.06% (D) CS-T: 14.35% (E) Hep-T: 22.19%.

Table 1. GC-T, HA-T, sHA-T, CS-T, Hep-T synthesis table

(A) Synthesis table of GC-T through DMTMM and (B) synthesis table of Tryramine conjugated polymers through EDC/NHS chemical reaction. All syntheses were calculated through the molar ratio of polymer and chemical.

A

	GC	DMTMM	4-hydroxyphenylacetic acid
Functional Group	[NH2]		[COOH]
Molar ratio	1	4	4

B

	HA, sHA, CS, Hep	EDC	NHS	Tyramine
Functional Group	[COOH]			[NH2]
Molar ratio	1	2	2	4

Table 2. Substitution degree (DS) of proton integration for polymer materials crosslinked with monophenol groups.

Material	Chemical shift (in ppm)	integral	H (mol)	Degree of substitution (%)
GC-T	Second carbon of GC peak(2.5-3.0 ppm)	1	1	16.59%
	Tyamine peak(6.8–7.5 ppm)	0.8297	4	
HA-T	Acteyl peak(2.0 ppm)	1	3	24.58%
	Tyamine peak(6.8–7.5 ppm)	0.3244	4	
sHA-T	Acteyl peak(2.0 ppm)	1	3	14.06%
	Tyamine peak(6.8–7.5 ppm)	0.1856	4	
CS-T	Acteyl peak(2.0 ppm)	1	3	14.35%
	Tyamine peak(6.8–7.5 ppm)	0.1894	4	
Hep-T	Acteyl peak(2.0 ppm)	1	3	22.19%
	Tyamine peak(6.8–7.5 ppm)	0.2929	4	

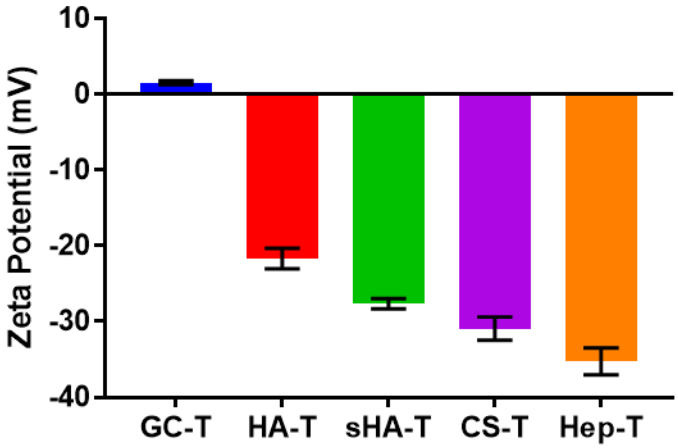

Figure 2.3 Zeta potential of 0.1% (w/v) GC-T, HA-T, sHA-T, CS-T, Hep-T.(n=3)

2.2.2 Reactivities of synthesized materials to SA-Ty

SA-Ty can be applied to functional groups with the oxidation of monophenols such as catechol (dopa) and ortho-Quinones (Figure 2.4) [25]. The reactivities of synthesized materials to SA-Ty were measured using a UV-Vis spectrometer. 0.1% (w/v) GC-T and HA-T, sHA-T, CS-T, and Hep-T dissolved in DW were used as substrates of SA-Ty, and $CuSO_4$ was also added. The concentration of GC-T, HA-T, sHA-T, CS-T, and Hep-T was determined based on the previous study [20]. The absorbance was measured at 475 nm (dopachrome = 3600 $M^{-1}cm^{-1}$) over time (Figure 2.5). The absorbance was compared 10 minutes after the enzyme reaction. GC-T had an absorbance of 0.061 ± 0.004 after 10 minutes of reaction to SA-Ty. HA-T was 0.074±0.001, sHA-T was 0.084±0.003, CS-T was 0.145±0.005, and Hep-T was 0.22±0.014. The color of the reaction solution turned brown within the reaction time. The aspect of this absorbance change provides that tyrosine is properly synthesized in the polymer and enzymatic reaction is performed according to SA-Ty. After fully reacting with SA-Ty, dia,lysis, and freeze-drying were performed, and Fourier transform infrared (FTIR) spectra were obtained using samples (Figure 2.6). After phenol oxidation, the peak of OH bonds increased at 3100-3500 cm^{-1}, and the C=O peak also increased at 1500-1800 cm^{-1}. This indicates that SA-Ty and monophenol group in polymers reacted and oxidized to catechol and *O*-quinone.

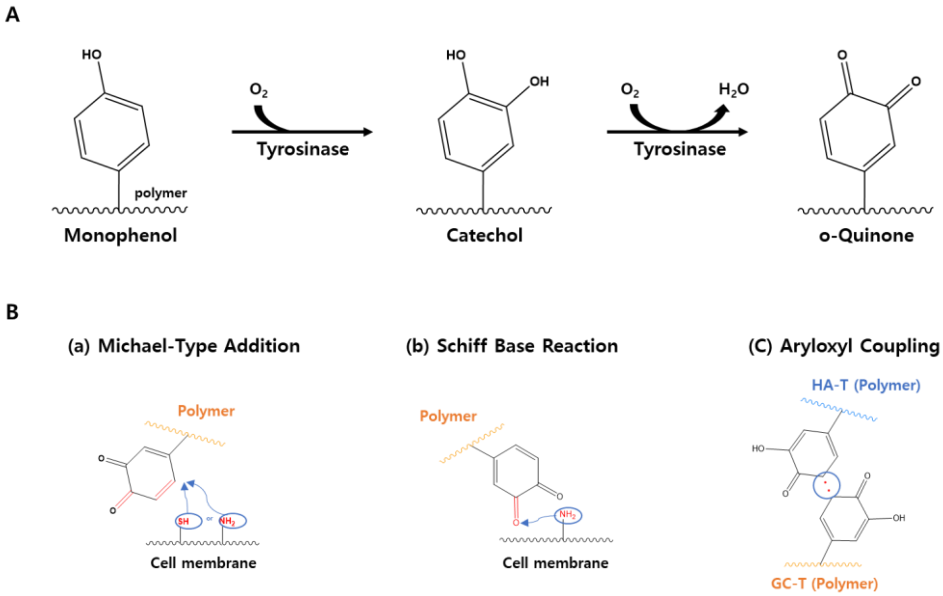

Figure 2.4 Oxidation reaction of monopoly by tyrosinase and consequent functional group change

(A) Monophenol of tyrosine is oxidized by oxygen and tyrosinase to catechol, o-quinone. (B) Reaction mechanism of nanofilm encapsulation.

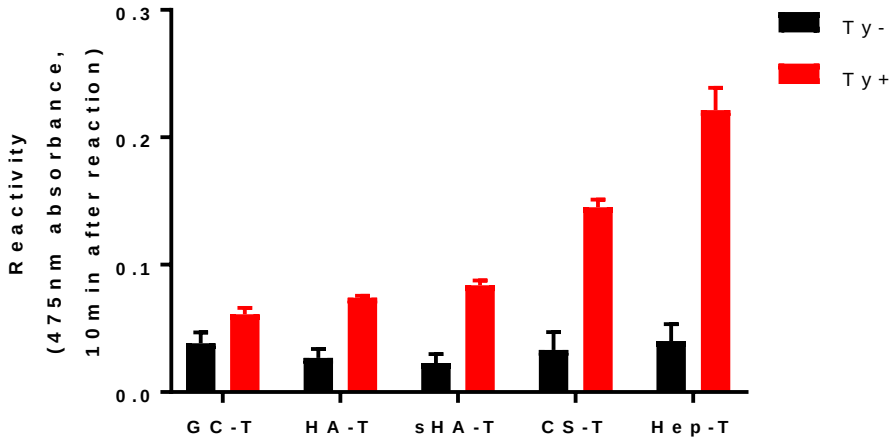

Figure 2.5 Enzymatic reactivity of SA-Ty reacted with 0.1% (w/v) materials 10 min after reaction.

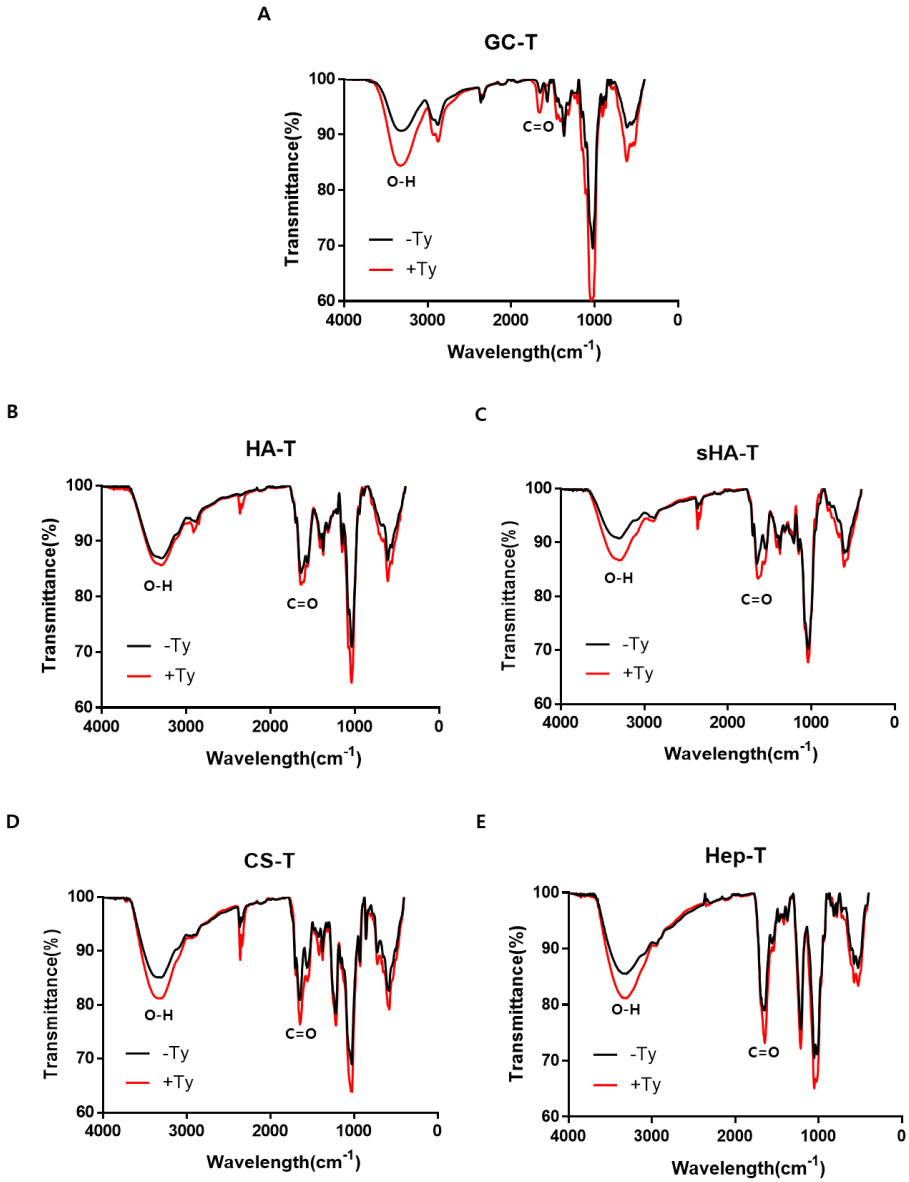

Figure 2.6 FTIR spectra of fully oxidized materials by SA-Ty.

2.2.3 Nanofilm-coated β-cell spheroids

β-cell spheroids were produced by seeding MIN6 cells in Aggrewell or ULA round-bottom 96 well plate (Figure 2.7). Spheroids were LbL coated in transwell using GC-T and HA-T via enzymatic crosslinking with SA-Ty until fifth layer as previously reported [20]. With the current platform, the sixth outermost layer was done using HA-T, sHA-T, CS-T, and Hep-T.

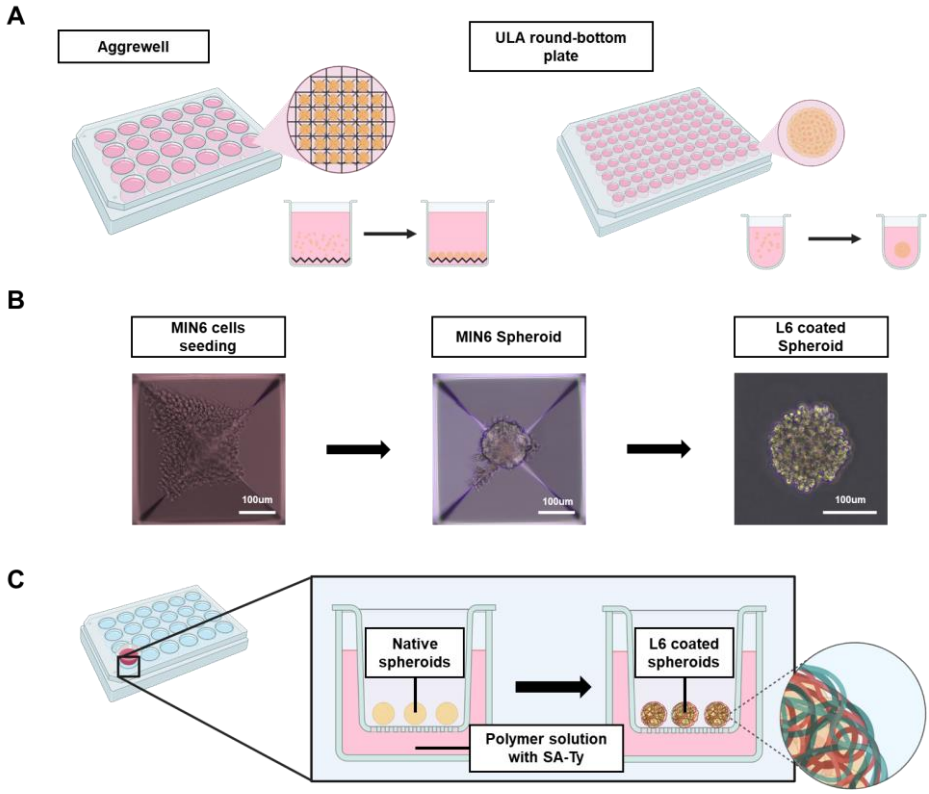

Figure 2.7 Layer-by-Layer (LbL)coating of spheroids from MIN6 β-cells.

(A) Schematic diagram of spheroid formation process using Aggrewell and ULA round-bottom plate. (B) Spheroid formation of MIN6 cells seeded in Aggrewell. (C) Schematic representation of LbL coating process.

2.2.4 Cell viability and Stability evaluation of hydrogel nanofilm coated β-cell spheroids

Cell viability was evaluated after LbL coating by staining β-cell spheroids with Calcein-AM and EthD-1 (Figure 2.8A). After coating up to 5 layers through the existing platform, the material expected to have an anticoagulant effect was applied to the sixth layer. Most cells were alive for seven days, regardless of the material, and only a few dead cells were identified on the spheroids as shown in (Figure 2.8A). Each synthesized polymer was confirmed to be non-toxic. Materials conjugated with FA (fluorescence amine) were coated on β-cell spheroids to evaluate the materials' coating stability (Figure 2.8B). The fluorescence images were obtained every 2 days from Day 0 to Day 6 after coating. As shown in Figure 2.8B., the fluorescence level was maintained after a week.

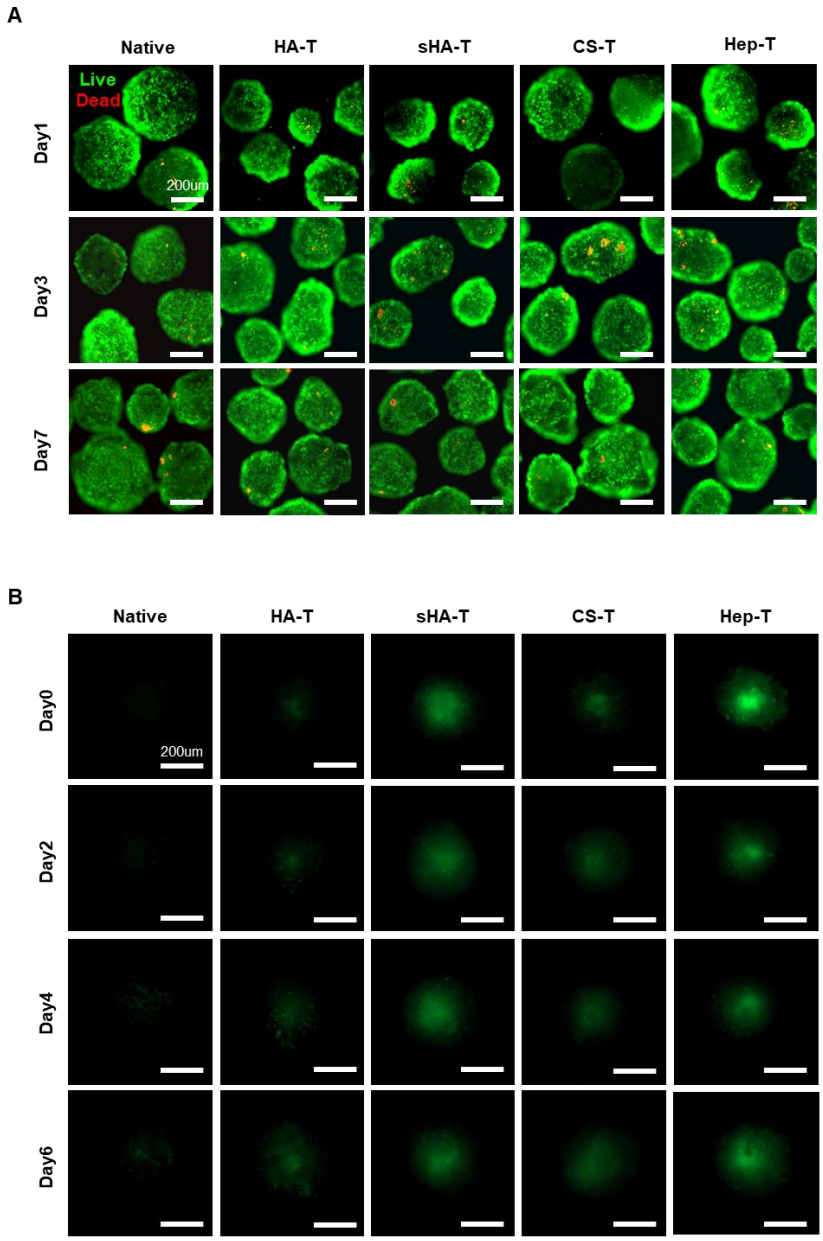

Figure 2.8 Cell viability and nanofilm coated β-cell spheroids stability evaluation.

(A) Live/dead assay images of native and outermost-layer-modified LbL-coated β-cell spheroids. (B)Fluorescence intensity of outermost-layer-modified LbL-coated β-cell spheroids measured every 2 days.

2.2.5 Coagulation test of material and coated beads

Clotting time was measured using platelet-rich plasma (PRP) to confirm the anticoagulant effect on the material (Figure 2.9-10). Since 0.1% (w/v) concentration was used in previous studies, 0.1% (w/v) concentration was used to measure the clotting time.

In order to clearly see the anticoagulant effect on the material, an experiment was conducted with a slightly higher concentration of 0.3% (w/v).Hep-T showed the longest clotting time compared to other materials, indicating a higher anticoagulant property of Hep-T (Figure 2.9). The anticoagulant effect of synthesized materials was further confirmed by coating the synthesized materials as the outermost on PMMA beads (Figure 2.10A). There were variations in clotting times depending on the material coated as the outermost layer on PMMA beads. Similar to the trend found in the clotting time of the material, Hep-T-coated beads showed the longest clotting time (Figure 2.10B). Therefore, among various materials, Hep-T shows the highest anticoagulant effect.

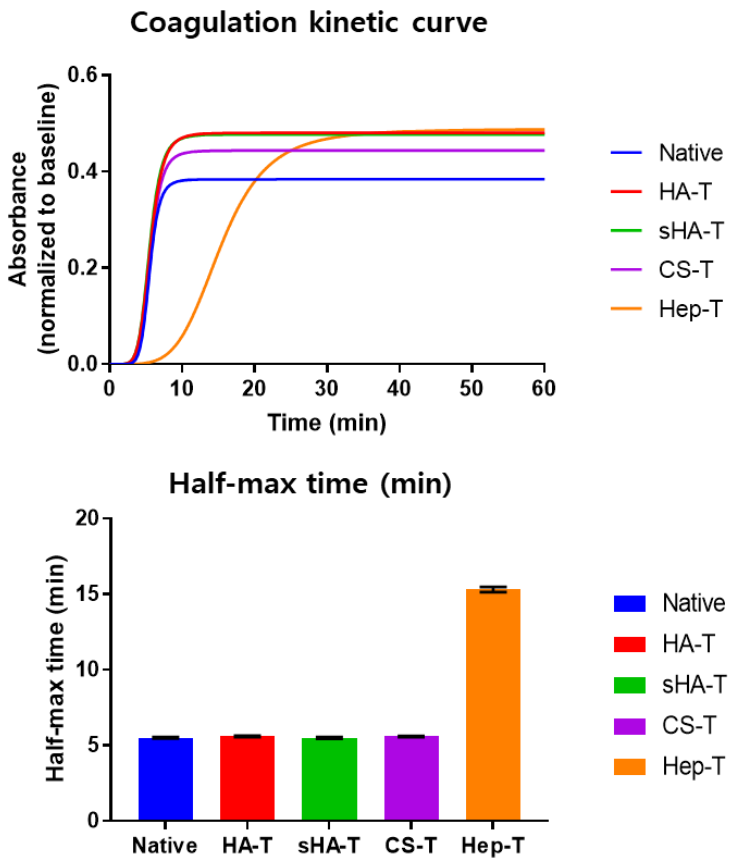

Figure 2.9 Coagulation test of polymers

Coagulation kinetics of polymers measured after incubation in PRP with 25mM $CaCl_2$ and Half-max clotting time measurement of polymers. (n=4)

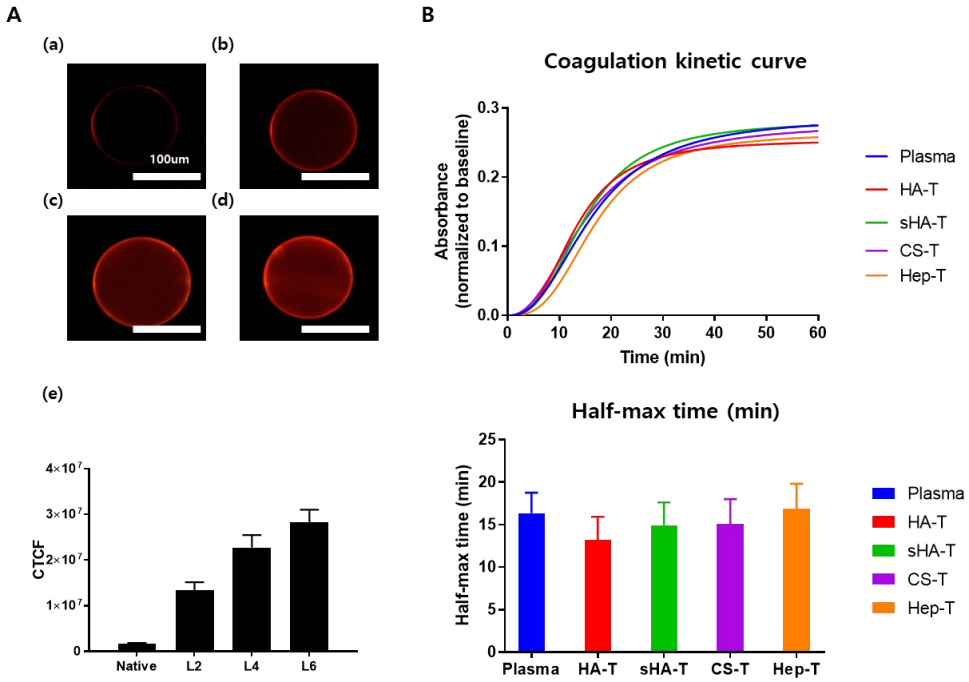

Figure 2.10 Fluorescence of Coated beads and Coagulation test of polymers coated bead.

(A)Fluorescence of Coated beads (a) Native (b) 2 layers (c) 4 layers (d) 6 layers-coated beads using GC-T-RITC (e) Quantitative fluorescence intensity of beads images. (B) Coagulation kinetics of polymer coated beads measured after incubation in PRP with 25mM $CaCl_2$ and Half-max clotting time measurement of polymer-coated beads. (n=4)

2.2.6 Platelet adhesion degree of coated material

The degree of attachment of the platelet was evaluated using silicon wafer and PDMS mold (Figure 2.11A). PDMS mold was attached to the Silicon wafer as shown in Figure2.11A. Then, the same volume of 0.5%(w/v) polymer solution and PRP were applied to the silicon wafer. The degree of attachment of the platelet was quantified by counting the number of platelets of 5 SEM images for each group (Figure 2.11C.). The degree of platelet attachment was found to be significantly lower in Hep-T coated sample compared to native Silicon wafer or HA-T coated sample. Hep-T with a low degree of platelet adhesion provides results that are effective in anticoagulation.

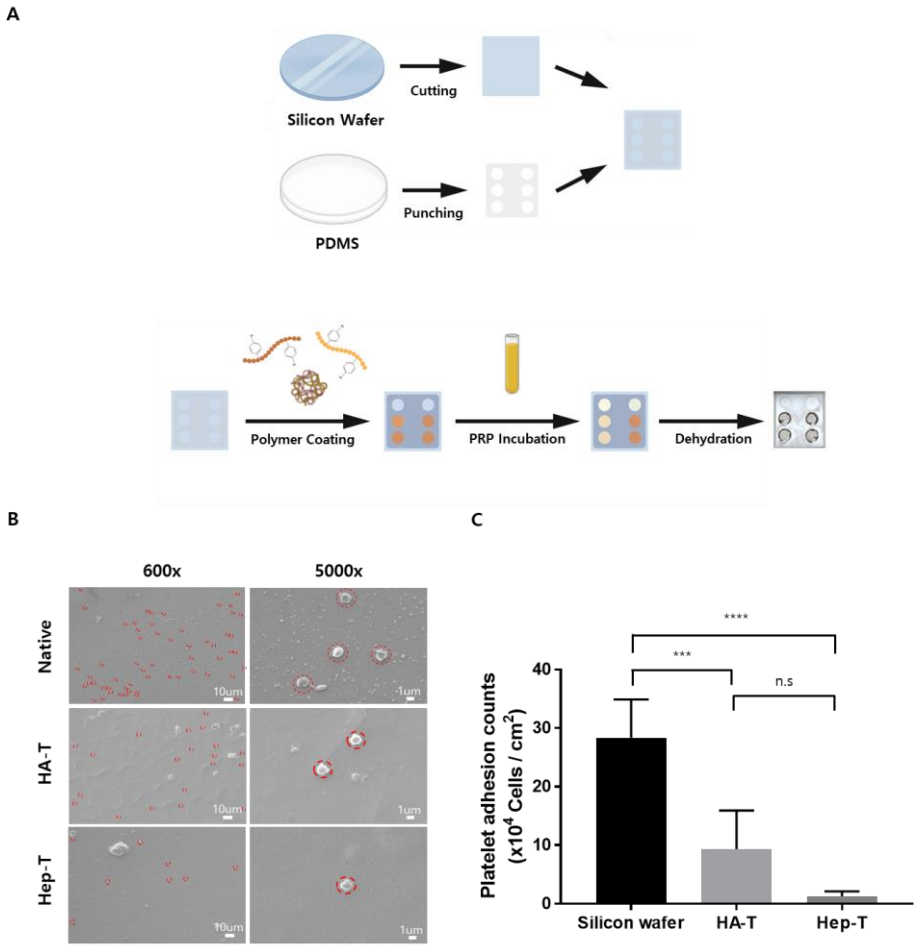

Figure 2.11 In vitro platelet adhesion test for SEM image.

(A) Polymers coated on the silicon wafer molded with PDMS were incubated with platelet-rich plasma and dehydrated in advance. (B) SEM image of platelet adhesion degree. (C) Platelet adhesion counts in 600X magnification panel (n=5).

2.2.7 Thrombin activity measurement of blood with nanofilm coated spheroids

Thrombin activity was measured after coating the synthesized materials (HA-T or Hep-T) as the outermost layer. After incubation of native, HA-T coated, and Hep-T coated spheroids in human whole blood, plasma samples were obtained, and a thrombin activity assay was performed. In addition, SEM images of spheroids were obtained and compared. Blood plasma incubated with Hep-T coated spheroids showed lower thrombin activity compared to blood plasma incubated with native and HA-T coated spheroids (Figure 2.12A). As shown in (Figure 2.12B), in the case of native spheroids incubated with human whole blood, the shape of spheroids was deformed after contact with blood. In the case of HA-T, the attachment of RBC to the spheroids was observed and the area surrounded by RBC was undergoing destruction. In the case of Hep-T, it was confirmed that fewer RBCs were attached to the spheroids, and the spheroids maintained their shape. These results showed that encapsulating β-cell spheroids with enzymatically cross-linked Hep-T outermost layer nanofilms lowers the activity of thrombin involved in blood coagulation.

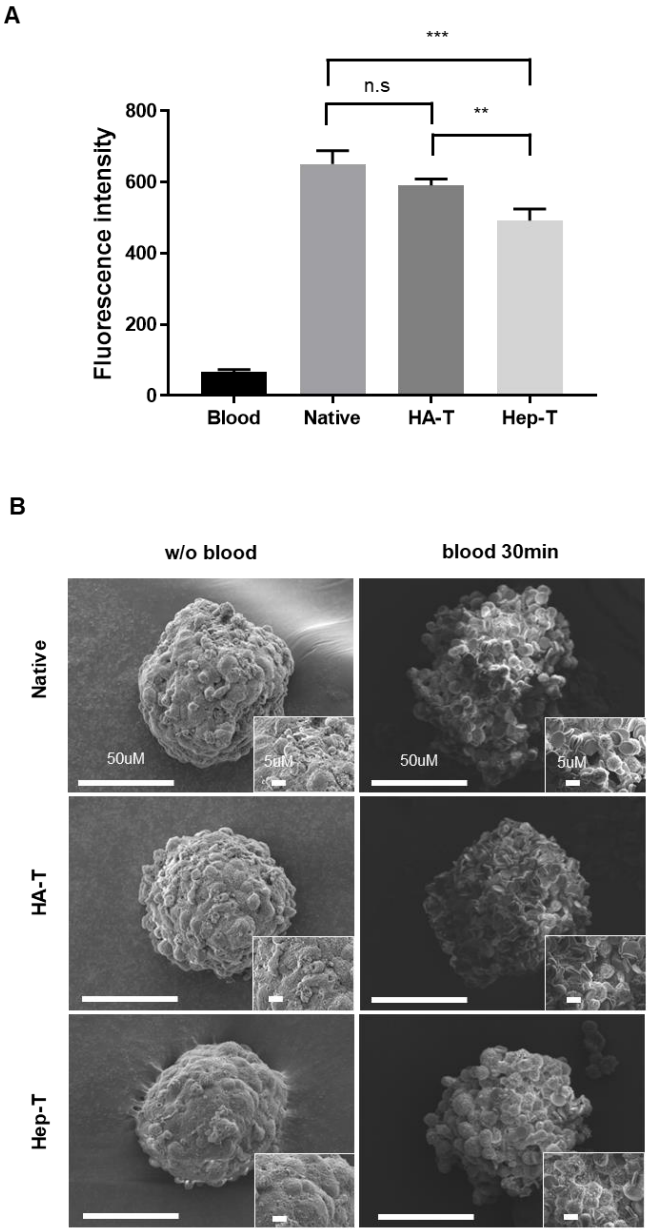

Figure 2.12 Thrombin activity measurement and SEM image of blood-incubated spheroids.

(A)Thrombin activity measurement (n=3). (B)SEM image of blood-incubated spheroids.

2.2.8 Evaluation of anticoagulant hydrogel film-coated β-cell spheroids function

Gene expression was evaluated via RT-qPCR and glucose-stimulated insulin secretion (GSIS) was performed on Native(N), HA-T coated (HA-T), and Hep-T coated (Hep-T) β cell spheroids to evaluate cell function (Figure 2.13A). There were no significant differences in β-cell function-related genes such as GLUT2, Ins-1, and Ins-2 between groups. To confirm GSIS, coated β-cell spheroids reacted in Krebs-Ringer solution containing low and high concentrations of glucose and proceeded to secrete insulin (Figure 2.13B). The secreted insulin level was normalized by dividing the total amount of insulin secreted by the amount of protein. The stimulation index (SI) was calculated by dividing the insulin level in the hyperglycemic solution by the insulin level in the hypoglycemic solution (Figure 2.13C). Insulin secretion was confirmed in Native spheroids, HA-T coated spheroids, and Hep-T coated spheroids. Overall, encapsulation of β cell spheroids with anticoagulant nanofilm did not interfere with β cell glucose sensitivity. Overall, encapsulation of *β*-cell spheroids with anticoagulant nanofilms did not interfere with the function and glucose sensitivity of β-cell cells, and these results suggest that Hep-T can be used as a new encapsulation material.

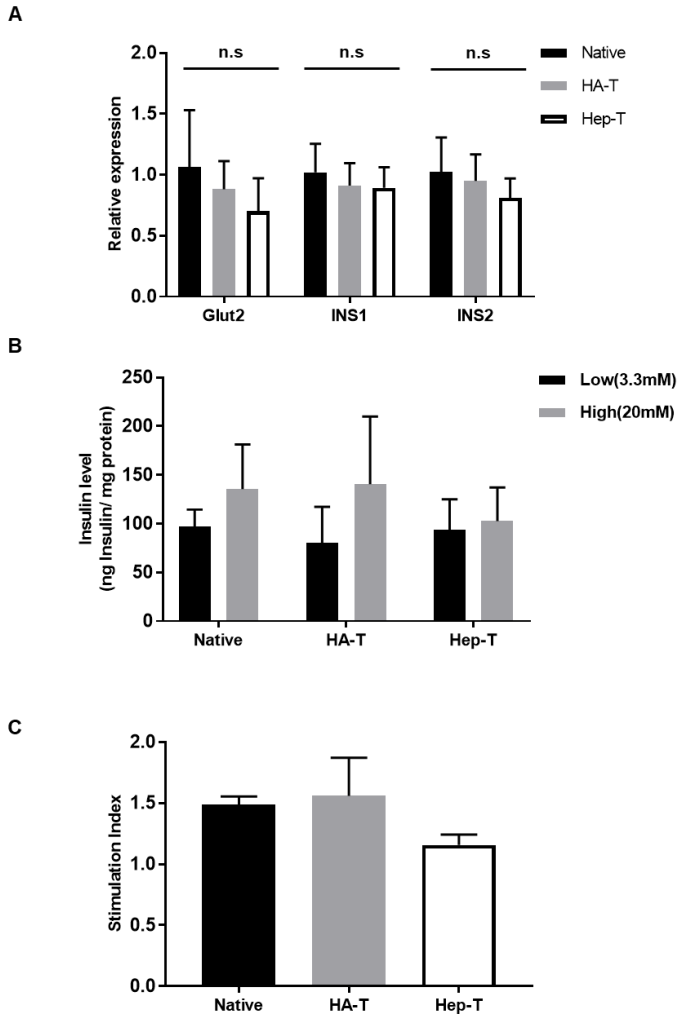

Figure 2.13 Evaluation of the functionality of anticoagulative outermost-layer-modified LbL-coated β-cell spheroids.

(A)β-cell marker comparison of through qPCR data analysis for native, HA-T, Hep-T coated spheroids (n=3). (B) Glucose-stimulated insulin secretion (GSIS) assay of β-cell spheroids at low (3.3 mM; black bar) and high (20 mM; gray bar) concentrations of glucose (n=2). (C) Stimulation index (SI) of GSIS Assay for native, HA-T and Hep-T coated β-cell spheroids (n = 2).

2.2.9 *In vivo* evaluation of engraftment and anticoagulation effects

After confirming the anticoagulating effect of Hep-T by lowering platelet adhesion and reducing thrombin activity using *in vitro* blood assays, *in vivo* evaluation was further carried out. The effect heparin (Hep-T) hydrogel nanofilms on the initial immune response was evaluated in a rat xenograft transplantation model (Figure 2.14). 3000 Hep-T L6 coated spheroids (Hep-T) were uniformly transplanted into liver via the ileocolic vein. For analysis, sham and native spheroids were injected as negative and positive control group respectively. Histological analysis confirmed engraftment of spheroids in both Hep-T and Native groups (Figure 2.15A). However, histological analysis showed no significant difference in the immune response. Additionally, the blood analysis of each group differed in TAT (Figure 2.15B). The group transplanted with Hep-T L6 coated spheroids showed a lower TAT value than the group transplanted with Native spheroids. However, there was no statistical significance. These results suggest that Hep-T might be effective in the reducing the initial blood coagulation and immune response. However, additional experiments and results with larger number of animals are necessary.

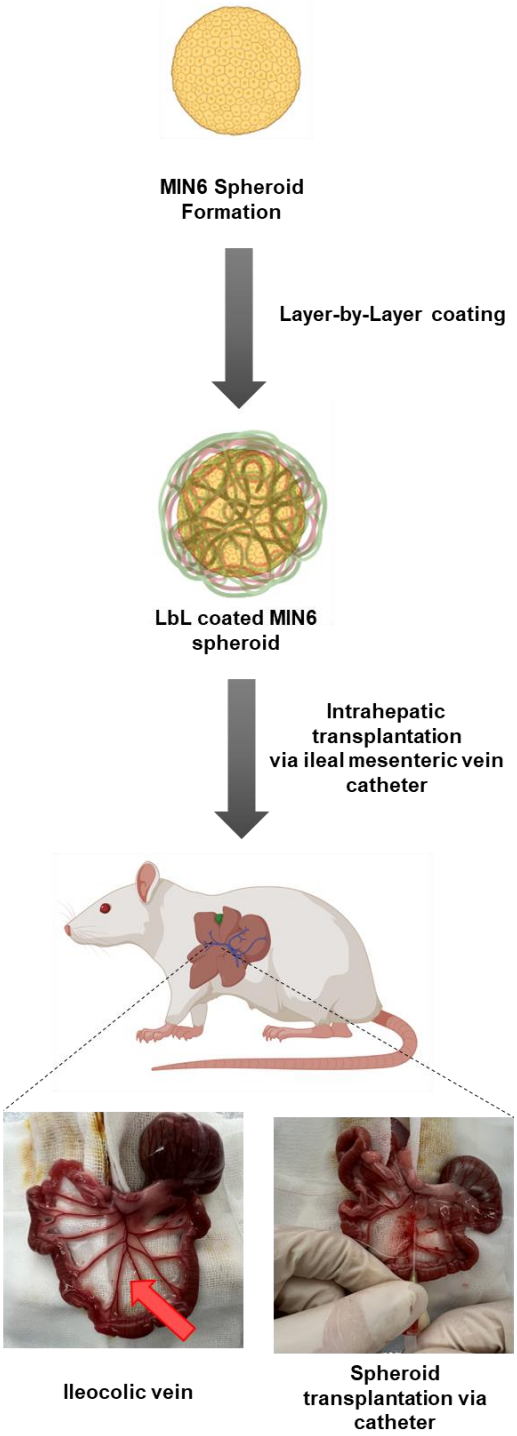

Figure 2.14 Transplantation scheme for encapsulated β-cell spheroid liver transplantation

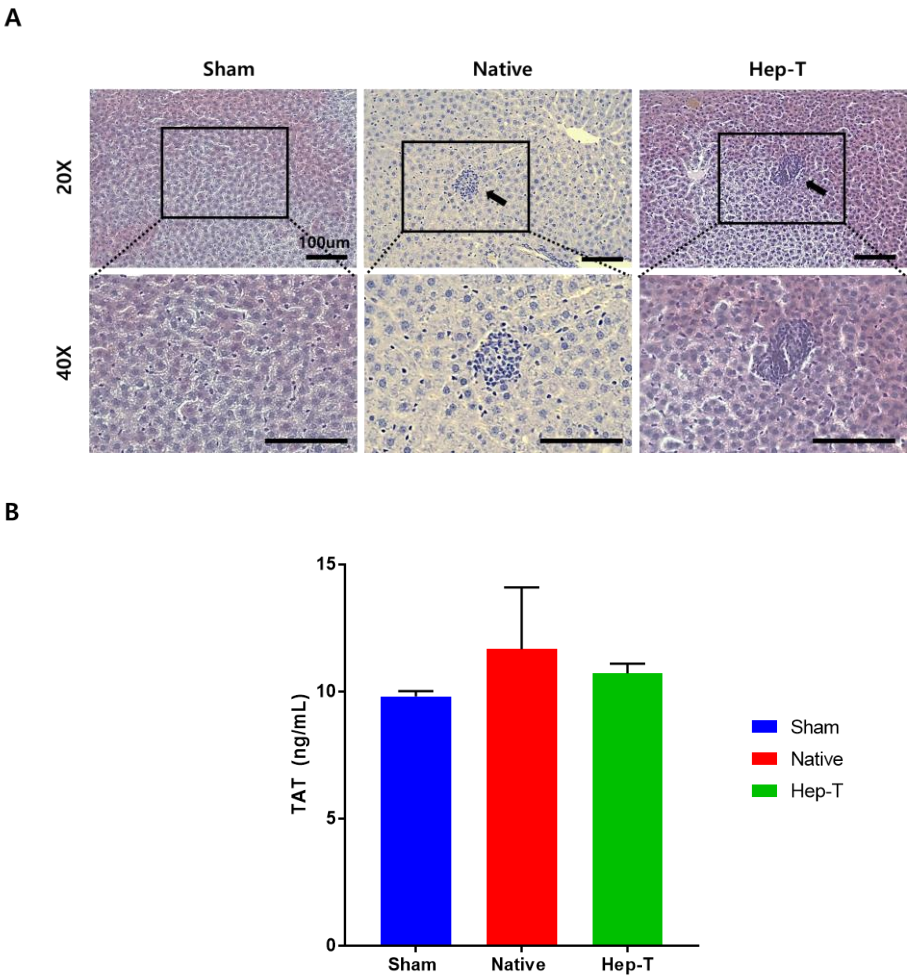

Figure 2.15 β-cell spheroids encapsulated with outermost anticoagulant nanofilm show anticoagulant effect in rat.

(A) Histological analysis of implants retrieved 3 days after implantation from rats, represented with hematoxylin and eosin (H&E) staining in each group. Scale bars, 100 μm (top images). (B) Anticoagulant evaluation on native, Hep-T coated β cell spheroids (n=2).

Chapter 3. Conclusion

This study has developed an anticoagulating nanofilm coating platform for a pancreatic islet transplant. Sulfated polymers including sulfated hyaluronic acid, chondroitin sulfate, and heparin were selected as candidates that are expected to have an anticoagulating effect. Monophenol was conjugated to sulfated polymers for the application of enzymatic crosslinking, and synthesized polymers were characterized. The cell survival rate was not affected when the synthesized sulfated polymers were applied to the outermost layer. Also, the stability of coated nanofilm was confirmed. The anticoagulating effect of synthesized sulfated polymers was evaluated by measuring the clotting time of platelet-poor plasma, and Hep-T showed significantly higher anticoagulating effects compared to other polymers. In addition, platelet adhesion and thrombin activity were measured, and it was confirmed that Hep-T induced less platelet adhesion and inhibited thrombin activity. Hep-T applied to the outermost layer of β-cell spheroid using enzyme crosslinking was confirmed to be engrafted when transplanted into rat liver, and blood analysis showed that it lowered thrombin-anti-thrombin reaction. Overall, our results describe an anticoagulating nanofilm coating that can potentially be applied to intrahepatic islet transplantation, and further applied to various cell transplantation that requires anti-coagulating function.

References

[1] J. Godwin, The promise of perfect adult tissue repair and regeneration in mammals: learning from regenerative amphibians and fish, BioEssays, 36 (2014) 861-871.
[2] M. Farina, J.F. Alexander, U. Thekkedath, M. Ferrari, A. Grattoni, Cell encapsulation: Overcoming barriers in cell transplantation in diabetes and beyond, Advanced drug delivery reviews, 139 (2019) 92-115.
[3] R. Krishnan, M. Alexander, L. Robles, C.E. Foster 3rd, J.R. Lakey, Islet and stem cell encapsulation for clinical transplantation, The review of diabetic studies: RDS, 11 (2014) 84.
[4] J. Kim, C.M. Hope, N. Gantumur, G.B. Perkins, S.O. Stead, Z. Yue, X. Liu, A.U. Asua, F.D. Kette, D. Penko, Encapsulation of human natural and induced regulatory T-cells in IL-2 and CCL1 supplemented alginate-GelMA hydrogel for 3D bioprinting, Advanced Functional Materials, 30 (2020) 2000544.
[5] L.M. Marquardt, S.C. Heilshorn, Design of injectable materials to improve stem cell transplantation, Current stem cell reports, 2 (2016) 207-220.
[6] N. Mitrousis, A. Fokina, M.S. Shoichet, Biomaterials for cell transplantation, Nature Reviews Materials, 3 (2018) 441-456.
[7] F. Duranti, G. Salti, B. Bovani, M. Calandra, M.L. Rosati, Injectable hyaluronic acid gel for soft tissue augmentation: A clinical and histological study, Dermatologic surgery, 24 (1998) 1317-1325.
[8] H. Cui, C. Liu, T. Esworthy, Y. Huang, Z.-x. Yu, X. Zhou, H. San, S.-j. Lee, S.Y. Hann, M. Boehm, 4D physiologically adaptable cardiac patch: a 4-month in vivo study for the treatment of myocardial infarction, Science advances, 6 (2020) eabb5067.
[9] L.A. DiMeglio, C. Evans-Molina, R.A. Oram, Type 1 diabetes, The Lancet, 391 (2018) 2449-2462.
[10] J.T. Warshauer, J.A. Bluestone, M.S. Anderson, New frontiers in the treatment of type 1 diabetes, Cell metabolism, 31 (2020) 46-61.
[11] M. Mobasseri, M. Shirmohammadi, T. Amiri, N. Vahed, H.H. Fard, M. Ghojazadeh, Prevalence and incidence of type 1 diabetes in the world: a systematic review and meta-analysis, Health promotion perspectives, 10 (2020) 98.
[12] P. Srinivasan, G. Huang, S. Amiel, N. Heaton, Islet cell transplantation, Postgraduate medical journal, 83 (2007) 224-229.
[13] A.J. Shapiro, J.R. Lakey, E.A. Ryan, G.S. Korbutt, E. Toth, G.L. Warnock, N.M. Kneteman, R.V. Rajotte, Islet transplantation in seven patients with type 1 diabetes mellitus using a glucocorticoid-free immunosuppressive regimen, New England Journal of Medicine, 343 (2000) 230-238.
[14] M. McCall, A.J. Shapiro, Update on islet transplantation, Cold Spring Harbor perspectives in medicine, 2 (2012) a007823.
[15] F. Cayabyab, L.R. Nih, E. Yoshihara, Advances in pancreatic islet transplantation sites for the treatment of diabetes, Frontiers in Endocrinology, (2021) 1077.
[16] I. Fujita, R. Utoh, M. Yamamoto, T. Okano, M. Yamato, The liver surface as a favorable site for islet cell sheet transplantation in type 1 diabetes model mice, Regenerative Therapy, 8 (2018) 65-72.
[17] V. Vaithilingam, B.E. Tuch, Islet transplantation and encapsulation: an update on recent developments, The review of diabetic studies: RDS, 8 (2011) 51.
[18] M.B. Oliveira, J. Hatami, J.F. Mano, Coating Strategies Using Layer-by-Layer Deposition for Cell Encapsulation, Chemistry–An Asian Journal, 11 (2016) 1753-1764.
[19] I. Kourtzelis, P.U. Magnusson, K. Kotlabova, J.D. Lambris, T. Chavakis, Regulation of instant blood mediated inflammatory reaction (IBMIR) in pancreatic islet xeno-transplantation: points for therapeutic interventions, Immune Responses to Biosurfaces, (2015) 171-188.
[20] M. Kim, H. Kim, Y.-s. Lee, S. Lee, S.-E. Kim, U.-J. Lee, S. Jung, C.-G. Park, J. Hong,

J. Doh, Novel enzymatic cross-linking–based hydrogel nanofilm caging system on pancreatic β cell spheroid for long-term blood glucose regulation, Science advances, 7 (2021) eabf7832.
[21] C.M.P.G. Dore, M.G.d.C.F. Alves, L.S.E.P. Will, T.G. Costa, D.A. Sabry, L.A.R. de Souza Rêgo, C.M. Accardo, H.A.O. Rocha, L.G.A. Filgueira, E.L. Leite, A sulfated polysaccharide, fucans, isolated from brown algae Sargassum vulgare with anticoagulant, antithrombotic, antioxidant and anti-inflammatory effects, Carbohydrate polymers, 91 (2013) 467-475.
[22] S.H. Lee, K. Baek, J.E. Lee, B.G. Kim, Using tyrosinase as a monophenol monooxygenase: A combined strategy for effective inhibition of melanin formation, Biotechnology and bioengineering, 113 (2016) 735-743.
[23] Y.-H. An, H.D. Kim, K. Kim, S.-H. Lee, H.-G. Yim, B.-G. Kim, N.S. Hwang, Enzyme-mediated tissue adhesive hydrogels for meniscus repair, International Journal of Biological Macromolecules, 110 (2018) 479-487.
[24] S.-H. Kim, S.-H. Lee, J.-E. Lee, S.J. Park, K. Kim, I.S. Kim, Y.-S. Lee, N.S. Hwang, B.-G. Kim, Tissue adhesive, rapid forming, and sprayable ECM hydrogel via recombinant tyrosinase crosslinking, Biomaterials, 178 (2018) 401-412.
[25] F. Panis, I. Kampatsikas, A. Bijelic, A. Rompel, Conversion of walnut tyrosinase into a catechol oxidase by site directed mutagenesis, Scientific reports, 10 (2020) 1-14.

국문초록

췌도 세포 이식용 항응고 나노필름 코팅 개발

췌도 이식에서 주요한계점은 이식 후 3일 이내 즉각적인 면역거부반응으로 인한 췌장기능 상실하는 것이다. 이식 후 췌도의 즉각적인 파괴를 막으려면 급성 혈액 매개 염증 반응을 완화하고 면역 체계를 억제해야 한다. 항응고 효과를 갖는 하이드로겔 나노필름의 재료로 항염증, 항응고 기능을 갖는 황산염이 도입된 고분자 및 황산염 고분자를 선정하였다. 모노페놀을 폴리머에 결합시키고 하이드로겔 나노필름은 Streptomyces avermitilis 유래 티로시나제(SA-Ty)를 매개로 한 모노페놀의 산화 반응을 통해 가교시켜 안정성을 높였다. 이식 초기 단계에서 발생하는 혈액 응고 및 급성 혈액 매개 염증 반응로부터 보호하기 위해 췌장 β 세포 회전 타원체의 표면에 항응고 하이드로겔 나노필름을 코팅하였다. 혈액 응고 방지 효과는 혈소판 유착, 트롬핀 활성을 측정하여 평가하였다. 항응고 하이드로겔 나노 필름은 베타 세포 스페로이드의 유전자 발현 정도 및 인슐린 분비능에 영향을 미치지 않았다. 이 코팅된 회전 타원체를 생체 내 쥐 모델에 이식하고 생착 및 항응고 효과를 평가하였다. 따라서, 본 연구에서 개발한 항응고 하이드로겔 나노 필름 코팅 기술이 제1형 당뇨병 치료를 위한 췌도 세포 이식에 있어 효과를 보일 것으로 기대한다.

주요어: 혈액 매개성 급성 염증반응, 헤파린, 혈액 응고 반응, 췌도 이식, 3D 세포 배양

학번: 2021-27001